Crystallization kinetics of a soda lime silica glass with TiO$_2$ addition

S.M. de la Parra-Arciniega, A. Álvarez-Méndez, L.C. Torres-González, and E.M. Sánchez*
Universidad Autónoma de Nuevo León,
Av. Pedro de Alba s/n, Cd. Universitaria, San Nicolás de Los Garza, N.L. 66400 México.

Studies conducted into Na$_2$O-CaO-3SiO$_2$ glass composition suggest that its phase transformation occurs from the surface towards the interior of the sample. In a study carried out in 1982, it was reported that no addition of nucleating agents modified the mechanism. Taking advantage of the disposition materials synthesized by nanotechnology, in this study TiO$_2$ in nanometer size was used with the idea that, because of its qualities, it could modify the crystallization mechanism. The glasses obtained as well as the thermally treated samples, were evaluated by the X-ray diffraction (XRD) powder method, differential thermal analysis (DTA), and by optical microscopy and high resolution transmission electron microscopy (HRTEM). Within the range of TiO$_2$ concentration studied (0 – 10 wt %), 10 wt % of TiO$_2$ considerably reduced the Na$_2$O-2CaO-3SiO$_2$ phase crystallization process. The crystallization mechanism was not modified and TiO$_2$ did not form compounds with the matrix components.

Keywords: Glass; crystallization; XRD; DTA; microscopy.

Estudios realizados en el sistema vítreo Na$_2$O-CaO-3SiO$_2$ sugieren que su transformación de fase ocurre desde su superficie hacia su interior. En estudios previos realizados se reportó la modificación del mecanismo de cristalización por adición de agentes nucleantes. En este estudio partículas nanométricas de TiO$_2$ fueron adicionadas con la idea de modificar el mecanismo de cristalización. Los vidrios obtenidos así como muestras tratadas térmicamente fueron evaluadas por difracción de rayos-X, análisis térmico diferencial, microscopía óptica y de transmisión electrónica de alta resolución. El rango de estudio realizado fue de 0-10 % en peso y se encontró que en la máxima adición se disminuyó considerablemente el proceso de cristalización. A pesar de la rápida disolución lograda por la adición de nanopartículas de titania no se logró un cambio del proceso de cristalización.

Descriptores: Vidrio calizo; cristalización; difracción de rayos-X; análisis térmico diferencial; microscopía.

PACS: 81.05.Kf; 81.05.Pj; 81.10.Jt

1. Introduction

When speaking of vitreous materials, an understanding is necessary of the factors that determine the speed of formation of the crystalline agglomerates and their speeds of growth, since this is a requirement in glass manufacturing, if the production of a homogenous product is desired. This is obtained through a study of crystallization kinetics, where parameters such as the crystallization mechanism and activation energy are to be found through models in which data obtained through microscopy methods and by isothermal and non-isothermal analysis (DTA and DSC) are used. The crystallization processes can be carried out on the surface and/or the volume of the glass.

The glasses of the Na$_2$O-CaO-SiO$_2$ system are used in diverse applications such as components of furniture, houses, automobiles, packages, etc. Nevertheless, its fragility is an aspect of technological and industrial interest, since it is to offer lasting and resistant articles to the use. What it has taken to the development of diverse techniques among are the addition of some metal either one or the more oxides of the alkaline type, alkaline earth or metallic. In this sense, the TiO$_2$ has conferred improvement in the mechanical properties of vitreous systems, having solved the problem of formation of cracks and which growth of surface crystalline layer is slowed down in its initial stage as happens in the CaO-P$_2$O$_5^1$and MgO-CaO-SiO$_2$-P$_2$O$_5^2$ systems, materials very im-

portant in the biological and industrial field to elaborate artificial bones and teeth [1].

Among the diverse studied compositions of soda lime silica glasses, it is Na$_2$O-CaO-3SiO$_2$, with 60% of SiO$_2$ content, on which Srtnad *et al.* [3] reported in 1973 that the crystallization process carried out from surface to the interior of the glass sample, this work was made under isothermal conditions and by microscopy. Ten years later, Saiello *et al.* [4] studied the same composition using non-isothermal method by differential thermal analysis (DTA) as well as Koga *et al.* in 1992 [5], and Ray and Day in 1996 [6], whom also concluded that crystallization was superficial. In 1982, Strnad published that this composition still did not crystallize in the volume neither with the addition of nucleating agents [7]. On the other hand, from mid the decade of the 80's, nanosize materials have been prepared with the remarkable quality that their properties are improved. In addition, although TiO$_2$ is one of the more common nucleating agents, its behavior not yet has been elucidated absolutely [8].

By such reason, the intention of this work was to prepare the glass of Na$_2$O-CaO-3SiO$_3$ composition with the addition of TiO$_2$, of nanometer size, in a range of 0-10 wt%. The obtained glasses and the effect of the heat treatments in the transformation of the phase were evaluated by X-ray diffraction, powder method; and the microstructure by optical microscopy and high resolution transmission electron microscopy (HRTEM). Also the effect of the TiO$_2$ was evalu-

Sample	Composition (wt %)			
	Na$_2$O	CaO	SiO$_2$	TiO$_2$
1	20.78	18.80	60.42	0
2	20.67	18.70	60.12	0.5
3	19.95	18.05	58.00	4
4	18.70	16.92	54.38	10

ated on the vitreous transition temperature, the vitreous stability against crystallization and the kinetic parameters of crystallization.

2. Experimental

The vitreous samples were prepared on the basis of the presented nominal composition in Table I. The reagents were mixed and they were ground in an agate mortar for 10 min, the mixture was put in a platinum crucible. In an electrical furnace, the CO$_2$ drive off was carried out at 900°C for half an hour, the fusion was at 1450°C for 3 hrs, then it was poured on a steel plate and it was pressed with another plate to obtain a piece of 2 ∼ 3 mm of thickness. The samples were analyzed by X-ray diffraction (XRD) powder method, in a Siemens D-5000 diffractometer, using radiation of Cu K$_\alpha$ ($\lambda = 1.5406$ Å) to confirm their amorphous state; their composition were evaluated by inductively coupled plasma (ICP), and they were analyzed by high resolution transmission electron microscopy.

A part of the sample was ground and sieved to a particle size < 53μm for thermoanalytical study conducted in differential thermal analysis (DTA) Shimadzu DTA50, for each measurement 10 mg of sample was put in a platinum cell with lid, air flow was (30 ml min^{-1}) and α-Al$_2$O$_3$ was used as reference.
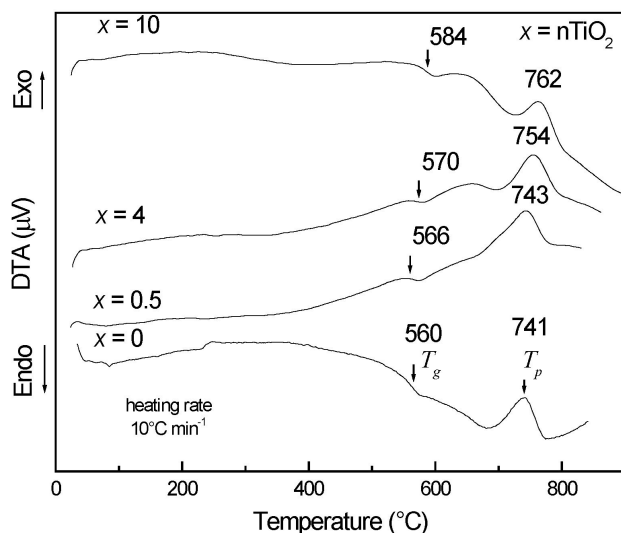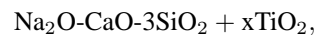

FIGURE 1. DTA curves of Na$_2$O-CaO-3SiO$_2$ + (0-10 wt %) nano-TiO$_2$ glass samples.

Once known the vitreous transition temperature, bulk glass samples of different compositions,

$$Na_2O\text{-}CaO\text{-}3SiO_2 + xTiO_2,$$

x = 0, 0.5, 4 and 10 wt%, were treated at the vitreous transition temperature for two hours to assure the maximum development nuclei, they were removed and cooled off on a refractory until room temperature, later they were introduced in the furnace to the temperature of crystallization avoiding that crystallized totally, again removed from the furnace and they were cool until room temperature. The samples thus obtained were used for the analysis of XRD and microscopy.

2.1. Characterization of the crystallized phases by X-ray diffraction

For XRD the samples were ground and they were mixed with internal standard of Si, then they were mounted on a steel plate. The measurements were made in a range of 2θ 5-90° with a step size of 0.01° and a counting time of 4.5 s for step. The crystalline phases were identified by means of the Joint Committee on Powder Diffraction Standards (JCPDS-ICDD) files.

2.2. Optical microscopy

The treated samples thermally were mounted in epoxic resin and polished until mesh 600. Then, slices of less than 1 mm of thickness were cut and they were washed with water in ultrasound by 20 min. Finally, each sample was mounted on a slide and it was polished with SiC in dust until having a so thin section that it revealed the microstructure, it was used a petrographic microscope with polarized light Leitz Laborlux 12 POL.

2.3. Kinetic parameters

The crystallization mechanism (n) was evaluated by the Ozawa's Eq. (9):

$$\frac{d\ln[-\ln(1-x)]}{d\ln\alpha} = -n, \tag{1}$$

where x is the fraction of crystallized volume and α is the heating rate, the value of 1 indicates surface crystallization, values from 2 to 4 indicate volume crystallization. The activation energy was determined by the method of Kissinger modified by Matusita and Sakka [10]:

TABLE II. Glass composition determined by ICP analysis.

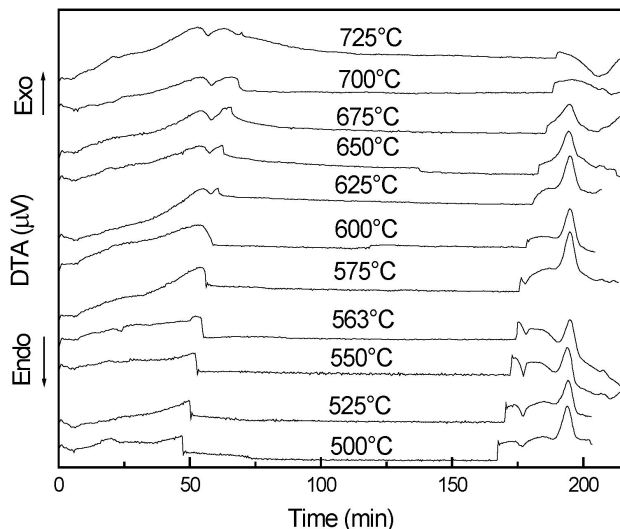| Sample	Composition (wt %)			
	Na$_2$O	CaO	SiO$_2$	TiO$_2$
1	20.50	19.20	59.80	0
2	20.30	19.10	59.40	0.50
3	19.40	18.00	57.80	3.89
4	18.75	17.60	53.60	9.49

FIGURE 2. DTA curves with double heating stage for the vitreous composition Na_2O-CaO-$3SiO_2$ + (10 wt %) nano-TiO_2. After h eating at $10°C$ min^{-1} from ambient temperature to nucleation temperature for 2hrs, it was then further heated until crystallization was complete.

$$\ln\left(\frac{\alpha^n}{T_p^2}\right) = -\frac{mE_a}{RT_p}, \qquad (2)$$

where T_p is the maximum temperature of crystallization peak, E_a is the activation energy for the crystalline growth, m is the dimensionality of the growth crystallization observed by microscopy and R is the constant of gases. Both are multiple-scan technique.

3. Results and discussion

The obtained glasses were transparent, homogeneous and colorless, also they were amorphous by X-ray diffraction. Table II reports the analysis of the composition of glasses carried out by ICP, the results present an inferior variation to 1% in weight. The curves of differential thermal analysis (DTA), for the four vitreous compositions Na_2O-CaO-$3SiO_2$+0, 0.5, 4 and 10 wt % nano-$TiO_2$are shown in Fig. 1, they present a single vitreous transition temperature, which indicates the existence of an amorphous state of homogenous composition [11]. Also it was registered that with the increase in the content of TiO_2, the vitreous transition temperature (T_g) was

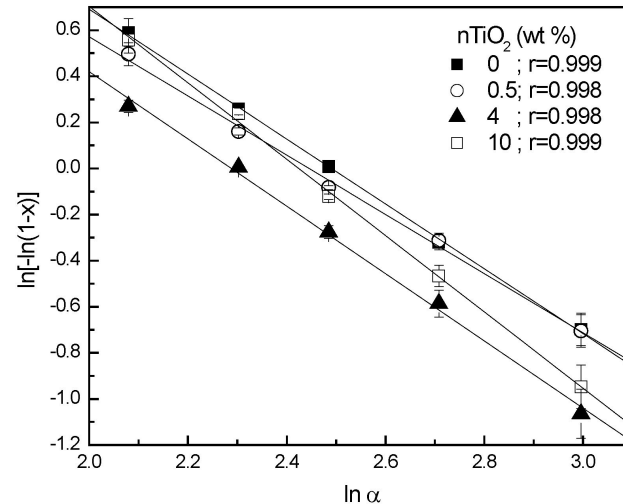

FIGURE 3. Graphs of $ln[-ln(1-x)]$ versus ln α for each of the nucleated samples in DTA of the vitreous system Na_2O-CaO-$3SiO_2$ + (0-10 wt %) nano-TiO_2.

increased gradually, this same behavior has been observed in other doped vitreous systems with metallic oxides [12,14]. TiO_2 behaves like intermediate oxide, that although is not able to form a glass, can take part in the vitreous network [15]. On the other hand, one exothermic event of crystallization only appeared in each curve. For the glass that does not contain nano-TiO_2 the temperature of peak crystallization was $741°C$, this value is among the range of temperature observed for this vitreous composition with particle size $<$ 100 μm studied by Koga *et al.* [5]. The exothermic peak moved to higher temperatures with the increase of the heat velocity; and for a given heat velocity the peak appeared to higher temperatures with the increase of TiO_2content, this behavior is the one that presented the system in which occurred surface crystallization such as Na_2O-$2SiO_2$ [16] and Li_2O-$2SiO_2$-$3TiO_2$ [17]. The glasses with 4 and 10 wt% of TiO_2 presented before peak crystallization a peak that simulates an endothermic transformation, which is related with the smoothed one of the glass that improves the contact of the sample with the cell. This behavior is consistent with the structure of the glass that becomes fragmented less with the increased of TiO_2. This was commented out by Saiello *et al.* [4], when they studied the soda lime silica glass system, increasing the SiO_2 content without additions.

TABLE III. Glass transition temperature (T_g), peak temperature (T_p), crystallization temperature (T_c) and ($T_c - T_g$), registered at a heating rate of $10°C$ min^{-1}.

TiO_2 (wt %)	T_g	T_p	T_c	$\Delta T = T_c - T_g$
0	560	741	701	141
0.5	566	743	708	142
4	570	754	713	143
10	584	762	733	149

TABLE IV. Values of the Avrami parameter (n), related to the crystallization mechanism.

Composition	Avrami parameter (n)
113	1.4 ± 0.02
113 + 0.5 wt % TiO_2	1.1 ± 0.04
113 + 4 wt % TiO_2	1.4 ± 0.05
113 + 10 wt % TiO_2	1.6 ± 0.03

TABLE V. Activation energy values (E_a) for the crystalline growth.

Composition	Activation energy, E_a (kJ mol^{-1})
113	333 ± 7
113 + 0.5 wt % TiO$_2$	308 ± 3
113 + 4 wt % TiO$_2$	312 ± 3
113 + 10 wt % TiO$_2$	359 ± 6

The vitreous stability against crystallization was determined by the difference $\Delta T = T_c - T_g$, where T_c is the extrapolated crystallization temperature and T_g is the vitreous transition temperature [18-19]. Results in Table III indicate that the glass Na$_2$O-CaO-3SiO$_2$ + 10% nano-TiO$_2$ is the most stable, with $\Delta T = 149°$C within the interval of glasses in study.

3.1. Nucleation curve and temperature of maximum nucleation rate

The range of temperature for the nucleation and the temperature for the maximum nucleation rate was determined from DTA curves (Fig. 2) for the glass most stable, Na$_2$O-CaO-3SiO$_2$ + (10 wt%) nano-TiO$_2$, the samples heated for 2 h at the temperatures indicated in Fig. 2. The criterion to select them was to begin from a temperature underneath the vitreous transition temperature (500°C) to a temperature within the crystallization region, (725°C). When the sample nucleus at 700°C the exothermic peak disappeared, this was attributed to the crystalline growth near this temperature. The temperature of maximum nucleation rate is when the height of crystallization peak is maximum [20], this occurred at 575°C.

3.2. Kinetic parameters

3.2.1. Crystallization mechanism

The graphs of $\ln[-\ln(1-x)]$ versus $\ln \alpha$ for each one of the compositions of the vitreous system Na$_2$O-CaO-3SiO$_2$ +(0-10 wt%) nano-TiO$_2$ appears in the Fig. 3, from whose adjustments by square minimums the value of the parameter of Avrami (n) was obtained from the slope. Results are reported in Table IV, in all the cases the value of n considers 1 what means that the crystallization of all the samples is surface and the crystal growth is towards the interior of the sample.

3.2.2. Activation energy

The graphs of $\ln(\alpha/T_p^2)$ vs $1/T_p$ appear in Fig. 4, from whose slopes the activation energy values (E_a) were obtained, the values are reported in the Table V.

For the samples with content of 0, 0.5 y 4 wt % nano-TiO$_2$ the activation energy values are ranged from 308 ± 3 to 333 ± 7 kJ mol^{-1}, but in the case of the samples with 10 wt% nano-TiO$_2$ the value is 359 ± 6 kJ mol^{-1}. The Ti^{4+} ion has high field strength, distributing an effect of ordering marked
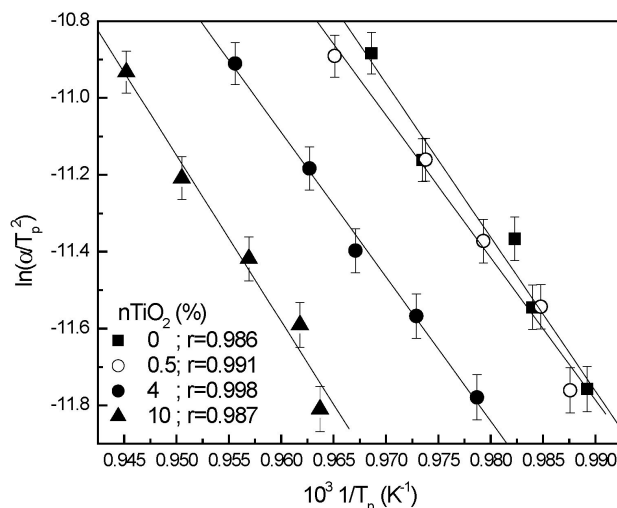

FIGURE 4. Graphs of $\ln(\alpha/T_p^2)$ versus $1/T_p$ for the nucleated samples of the system Na$_2$O-CaO-3SiO$_2$ + (0-10% wt) nano-TiO$_2$, from which the values of activation energy (E_a) are derived.
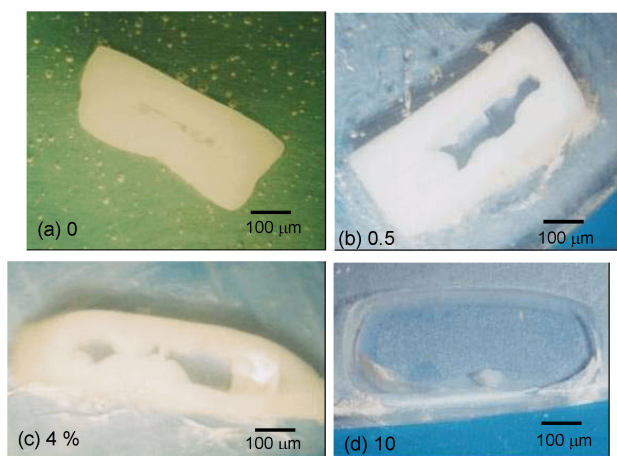

FIGURE 5. Samples 113 + nano-TiO$_2$, (a - d) treated at 575°C / 2h and 800°C / 1.5 h. Amplification 8X.
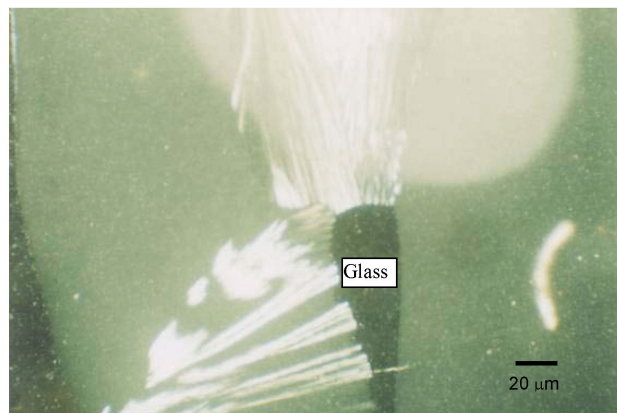

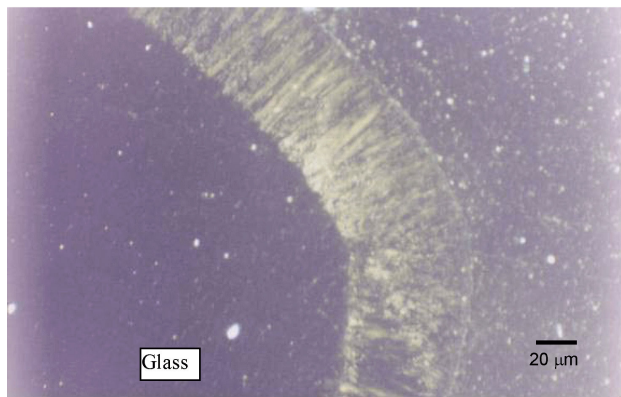FIGURE 6. Na$_2$O-CaO-3SiO$_2$ (nucleation: 575°C / 2h and crystallization: 800°C / 1.5h). Amplification 40X.

FIGURE 7. $Na_2O-CaO-3SiO_2$ + 10 % nano-TiO_2 (nucleation: $575°C$ / 2h and crystallization: $800°C$ / 1.5h). Amplification 40X.

in glasses. This can be the reason for the high value of the activation energy in the composition with 10 wt% nano-TiO_2 [21]. Koga *et al.* [5] made non-isothermal study of $Na_2O-CaO-3SiO_2$ varying the particle size, and for a particle size < 100 μm the temperature range of the peak crystallization was 698 - 773°C and the activation energy was 303 ± 7 kJ/mol. In addition they observed that if the temperatures of the peak crystallization fell over 800°C the values of E_a showed a constant value around 250 kJ/mol, this result was similar to the obtained one by the isothermal method made by microscopy in 70's [3]. Alizadeh and Marghussian [22] and Hu and Huang [23] indicated that the activation energy for a crystallization of surface type is generally smaller than for a volumetric crystallization. Although the content of nano-TiO_2 that was handled did not change the crystallization mechanism, it diminished the crystal growth; and the values of the activation energy are more similar to the one that is reported for the crystallization of the $Na_2O-2CaO-3SiO_2$ glass (E_a = 357 kJ/mol) [24] that presented a volumetric mechanism.

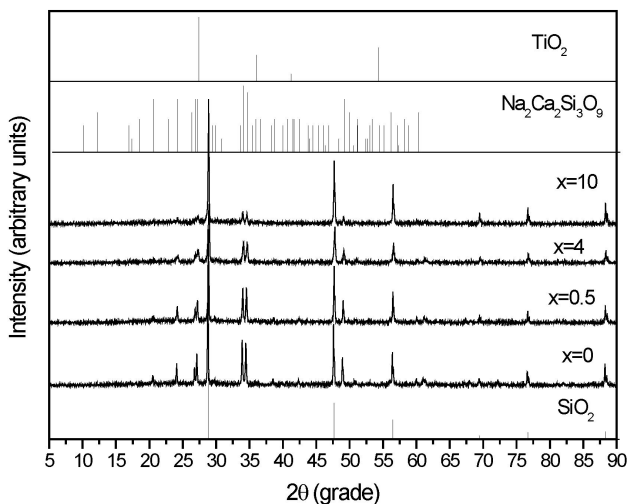FIGURE 8. X-ray diffraction patterns of the glass samples Na_2O - $CaO-3SiO_2$ + (0-10 wt %) nano-TiO_2 treated thermally.
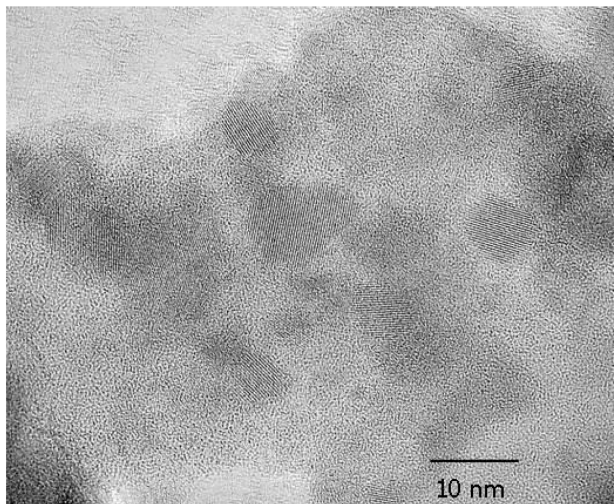

FIGURE 9. HRTEM micrograph of $Na_2O-CaO-3SiO_2$ + 4 wt% nano-TiO_2 sample glass showing nanocrystals of TiO_2.

In this glass the temperature of maximum nucleation rate is around the vitreous transition temperature, which indicates that the glass is nucleated totally before the process of crystalline growth occurs. It was determined by optical microscopy that the thickness of crystals diminished as the concentration of TiO_2 increased (Fig. 5). The crystals display rod type form, their growth is perpendicular to the surface and towards the interior of the sample, some agglomerate ones show to have grown like a branch (Figs. 6 and 7). The morphology and the direction of these crystals indicate that the surface crystallization taking starts off in a preferential direction. These results agree with the results obtained by the thermoanalytical study, in which, by the Ozawa method it was obtained that the crystallization mechanism is of surface type.

3.2.3. XRD analysis

Fig. 8 shows the X-ray diffraction patterns of the samples 113+0, 0.5, 0.4 and 10 wt% nano-TiO_2. The hump between 15 and 27° (2θ) represents the existence of vitreous phase. The reflection at 28° corresponds to the internal standard of Si (ICDD, #27-1402). In these diffraction patterns the reflections at 33.6°, 34.2° and other lines corresponding to the phase $Na_2Ca_2Si_3O_9$ (123) were identified (ICDD, #22-1455), also a peak in 27.4° (2θ) was identified and corresponds to the most intense line of TiO_2 (rutile) phase (ICDD, #21-1276).

3.2.4. HRTEM analysis

By high resolution transmission electron microscopy (HRTEM) the precipitation of TiO_2 to nanometric size was determined. In Fig. 9 a micrograph of the $Na_2O-CaO-3SiO_2$ glass with 4 wt% nano-TiO_2 is shown, where there are nanoparticles immersed in the vitreous matrix; their sizes are 10 nm approximately, one third of the very high average for the reagent. This indicates that the TiO_2 in the sam-

ple dissolved during fusion. The spacing between fringes is 2.97±0.05 Å, which corresponds to parameter c of rutile with a tetragonal structure and with cell parameters $a = 4.5933$ Å and $c = 2.9592$ Å (ICDD, #21-1276).

4. Conclusions

The influence of TiO$_2$ on the crystallization kinetics of Na$_2$O-CaO-3SiO$_2$ glass was investigated. As TiO$_2$ changes from 0 to 10 wt %, the glass transition temperature (T_g) and the temperature of crystallization (T_p) increase, indicating that TiO$_2$ acts as an inhibitor of the crystallization process in this system, an effect that is more evident in the glass with 10 wt%.

The crystallization process was evaluated by an isothermal method and optical microscopy, as well as by a non-isothermal method. These studies corroborate a surface crystallization process. The activation energy value, E_a, corresponds to the crystallization of the Na$_2$O-2CaO-3SiO$_2$ phase. By HRTEM, it was determined that the vitreous samples display a uniform distribution of nanocrystalline particles of TiO$_2$.

Acknowledgements

∗. Corresponding author. Tel.: +52 81 83 29 40 10 ext. 6242; fax: +52 81 83 76 53 75, e-mail address: info_labiv@yahoo.com

1. Lee, Jinn-Shing, Hsu, and Chung-King, *Thermochim. Acta* **333** (1999) 115.

2. Shyu, Jyh.-Jiin, and Wu Jenn-Ming, *J. Mater. Sci. Lett.* **10** (1991) 1056.

3. Z. Strnad and R.W. Douglas, *Phys. Chem. Glasses* **14** (1973) 33.

4. S. Saiello, F. Branda, A. Buri, and A. Marotta, *Verres Réfract.* **36** (1982) 859.

5. N. Koga, J. Sestak, and Z. Strnad, *Thermochim. Acta* **203** (1992) 361.

6. C.S. Ray and D.E. Day, *Thermochim. Acta,* **280/281** (1996) 163.

7. Strnad and Zdenek, *Glass-Ceramic Materials* (1986) 72.

8. Duan, Ren-Guan, Liang, Kai-Ming, and Gu Shou-Ren, *J. European Ceramic Society* **18** (1998) 1729.

9. T. Ozawa, *Kinetics of non-isothermal crystallization. Polymer* **12** (1971) 150.

10. K. Matusita and S. Sakka, *J. Non-Cryst. Solids* **38** (1980) 741.

11. Hsi, Chi-Shiung, Wang, and Moo-Chin, *J. Mater. Res.* **13** (1998) 2655.

12. Lee, Jinn-Shing., Hsu, and Chung-King, *Thermochim. Acta* **333** (1999) 115.

13. Lederer, Kay., Deckwerth, M. Rüssel, and Christian, *J. Non-cryst. Solids* **224** (1998) 103.

14. Fisher *et al.*, *J. Non-Cryst. Solids.* **351** (2005) 623.

15. P.W. McMillan, *Glass-Ceramics*, Second Edition. (Academic Press, Great Britain, 1979) p. 14.

16. Wakasugi, Takashi, Ota, and Rikuo, *J. Non-Cryst. Solids* **274** (2000) 175.

17. K. Matusita, S. Sakka, and Y. Matsui, *J. Mater. Sci.* **10** (1975) 961.

18. Weinberg and C. Michael, *J. Non-Cryst. Solids* **167** (1984) 81.

19. M.M. Wakkad, *J. Thermal Analysis and Calorimetry* **63** (2001) 533.

20. C.S. Ray and D.E. Day, *Nucleation and crystallization in liquids and glasses* (1993) 207.

21. N. Lahl, K. Singh, L. Singheiser, K. Hilpert, and D. Bahadur, *J. Mater. Sci.* **35** (2000) 3089.

22. P. Alizadeh and V.K. Marghussian, *J. Eur. Ceram. Soc.* **20** (2000) 775.

23. Yi Hu and C.L. Huang, *J. Non-Cryst. Solids.* **278** (2000) 170.

24. X.J. Xu, C.S. Ray, and D.E. Day, *J. Am. Ceram. Soc.* **74** (1991) 909.